Experimental Results and Numerical Simulation on the Ion Space Charge Formation

C. Agheorghiesei, G. Popa and R. Schrittwieser[1]

Faculty of Physics, University „Al. I. Cuza", Blvd. Carol I 11, RO-6600 Ia°i, Romania
[1]Institute for Ion Physics, Innsbruck University, Technikerstr. 25, A-6020 Innsbruck, Austria
ghpopa@uaic.ro

Abstract.

Experimental results and numerical simulations are presented on ion-space charge instabilities excited in a DP-machine. The space charge is formed in one chamber when the ions are injected from the plasma chamber through the separating grid. The experimental conditions are specified, in which a steady state space charge is formed, and the conditions, when the space charge becomes unstable. The space-time distribution of the ion density within the ion space charge is presented during its coherent oscillation. Between experimental results and numerical simulations by the PDP1-code good agreement has been obtained.

Introduction.

Space charge structures have been investigated since the beginning of the last century [1,2] for planar diodes assuming a Maxwellian distribution of the particles entering the diode. The interest on the subject strongly rose, when thermionic converters [3,4] and the origin of the oscillations in such a system [5,6] were investigated. A very important extension of the subject was made when Q-machines [7] started to be used. For about two decades electrostatic instabilities were investigated in such a diode plasma system and both, analytical models [8] and particle simulations [9] have shown that the system must be considered as a bounded plasma, in which also the external circuit is important [10].

In contrast to diode and Q-machine plasmas, where Maxwellian distributions of the particles are assumed, in this paper the boundary conditions are different. The ions enter the diode almost as a monokinetic beam with a high speed and large density, compared to the electrons, which enter the diode through the same surface but at very low density and almost thermal velocity. This situation corresponds to the one-grid electrostatic analyser [11] and a one-grid ion source system [12].

Experimental set-up

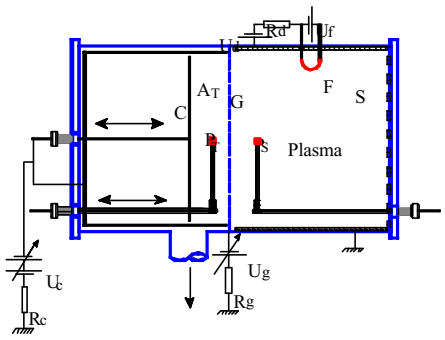

Fig. 1: Experimental set-up

The experiments have been performed in the DP-machine of the Innsbruck University [1]. The experimental set-up is presented in Fig. 1. An argon plasma is produced in the source chamber (S) by a DC discharge between a negatively biased tungsten filament (F) (U_D = -50V) and a grounded anode (the wall chamber). The argon pressure was kept constant at 10^{-4} mbar. The plasma parameters were: a density between $3\cdot10^{7}$ and $3\cdot10^{8}$ cm^{-3}; an electron temperature of T_e = 3,2 eV; ion temperature of T_i = 0,15 eV. The ions may enter the target chamber T through the separating grid (G) (stainless steel, 77 wires/cm and a geometrical transparency of 48%).

The grid bias was negative enough (U_G between –80 and –300 V) to prevent electrons from the source chamber to enter the target chamber. In spite of that electrons were present in the target chamber because of secondary electron emission from the grid wires due to ion bombardment. The length d of the target chamber was varied between 5 and 200 mm using an axially movable disk electrode (42 cm in diameter) as collector (C).

The cylindrical target chamber was similar to a one- grid electrostatic analyser, which is limited on one side by the grid and an other side by a cylinder A_T and the collector C, which can be biased separately or together. The latter was the situation in the experiments, and so the collector bias was U_C with respect to ground. Both, grid current (I_G) and collector current (I_C) were measured.

The plasma parameters and parameters of the ion space charge were measured using the electrostatic plane probes P_S in the source chamber and P_T in the target chamber, respectively. The fluctuations of both currents, i.e., I_G and I_C, were registered and analysed using a digital oscilloscope.

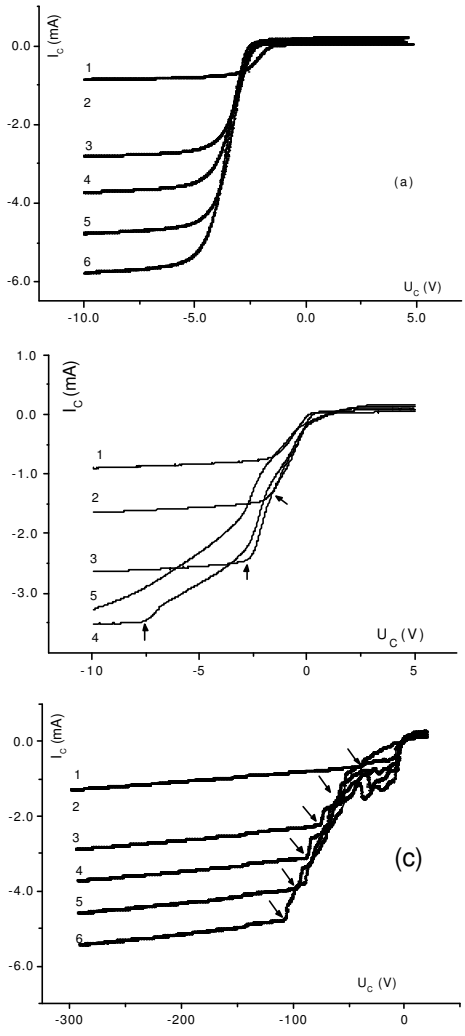

Fig. 2 Current-voltage characteristics $I_C(U_C)$ for grid-collector distance of: a) 3mm, b) 20mm c) 90mm. Plasma density parameters curves:
1 – 3,2·10^7 cm^{-3} 2 - 5,7·10^7 cm^{-3}
3 – 8,2·10^7 cm^{-3} 4 – 1,1·10^8 cm^{-3}
5 – 1,3·10^8 cm^{-3} 6 – 1,6·10^8 cm^{-3}

Space-time distributions of the ion-space charge parameters in the target were registered using the box-car system and axially movable probe P_T.

Experimental results and discussions

The target chamber, presented in Fig. 1 on the left-hand side, is in this experiment used as "diode" system. Whereas the grid bias prevents electrons to enter from the source chamber into this diode, ions can enter as a beam, the density of which is varied by changing the plasma density in the source chamber. The ions can be collected or reflected by C according to its bias, but their presence in the "diode" has a strong influence on the spatial distributions of both, the electrostatic potential and the ion space charge density. This influence was observed as a modification of the current voltage characteristic $I_C = I_C(U)$ of the collector and of the ion density between G and C.

In Fig. 2 three families of $I_C(U_C)$ characteristics are presented having as parameters both, the plasma density (curves 1 to 6) and the distance d between C and G. For higher densities and larger distances the system can become unstable (Fig. 2b and 2c), when U_C surpasses a certain threshold. As long as d is small (on the order of the Debye length) there are no conditions for an ion space charge formation and the $I_C(U_C)$ characteristics show a monotonic behaviour as it is known from electrostatic analysers (Fig. 2a). With increasing diode length d, the ions can change the monotonic dependence of I_C on U_C. In Fig. 2b and c, arrows indicate the instability threshold, which corresponds also to the on-set of the ion saturation current to the collector C.

The unstable behaviour appears as oscillations

of both, the grid ($\tilde{I}_G$) and the collector ($\tilde{I}_C$) current, the former with small amplitudes, so that $\tilde{I}_G/\bar{I}_G$ < 0,1, while in the latter case the relative amplitude $\tilde{I}_G/\bar{I}_G$ might reach values up to 0,8 (where $\bar{I}_G$ and $\bar{I}_C$ are the mean values). Moreover, these oscillations may change between 3 or 4 different modes depending on the collector bias, which was varied between the two saturated regions of the $I_C(U_C)$ characteristics, and for a distance d larger than about 20mm.

One oscillatory mode appears for U_C around the plasma potential in the source chamber so that almost all ions are reflected back towards the source chamber. Some characteristics of the system in this regime were previously presented [11]. In this case a typical $I_C = I_C(U)$ characteristic shows a large hysteresis as presented in Fig. 3a, while the axial ion saturation current of the probe between G and C shows a maximum ion density near the grid.

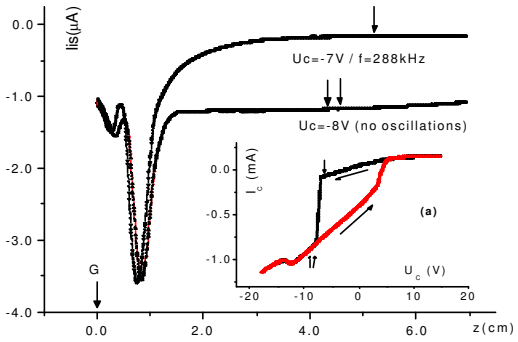

Figure 3: Axial distributions of the probe ion saturation current between the grid (G) and the collector (C) for the unstable regime (labelled ↓) and the stable one (↓↓). The corresponding $I_C(U_C)$ characteristic is plotted in (a)

There are two axial distributions of the probe ion saturation current I_{is}. One corresponds to the steady state system (U_C = –8 V, Fig. 2), and the other one to the presence of large current oscillations (U_C = –7 V, Fig. 2). In the latter case the mean value of the probe current was registered.

There are three main characteristics of these axial distributions that were investigated in this paper both experimentally and by simulations:

a) There is, in general, a double peak structure of the axial distribution of I_{is}. The two peaks behave differently with the probe bias. One peak preserves its position with respect to the grid but its value strongly changes, while the other peak changes its position but is less sensitive to the bias of the probe (Fig. 4). The former peak was identified as the position of the ion space charge formation near G, while the latter one is a result of trajectories of the ions because of the probe bias.

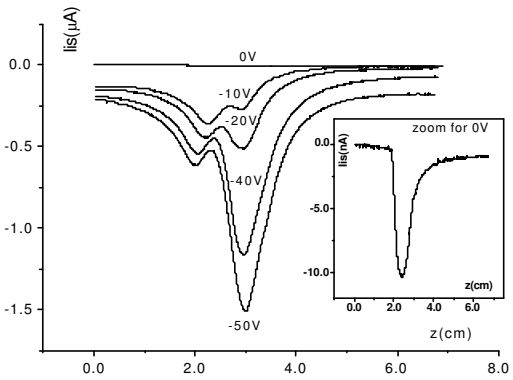

Figure 4: Axial distributions of the probe saturation ion current between G and with the grid bias as parameter.

b) Both peaks do not change significantly when the diode passes from the stable to the unstable regime. This fact shows that oscillations are not localised in the space charge region.

c) There is a strong decrease of I_{is} in the region between the space charge and the collector when the diode passes into the unstable regime compared to the steady state one. In order to illustrate this characteristic, the axial distribution of ion (Fig. 5a) and electron (Fig. 5b) probe saturation currents are presented for different instants during one period of the collector oscillation (Fig. 5c). Both currents are comparable and show strong oscillations which represent a PRI behavior [11].

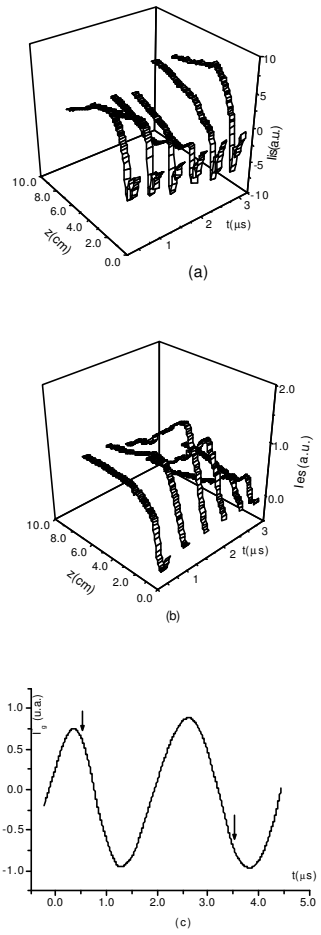

Figure 5: Axial distribution of the both ion (a) and electron (b) currents of the probe between G and C at different instant time during one period of oscillation (c)

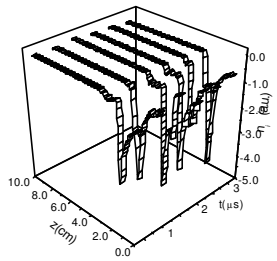

Fig. 6: Axial distribution of the ion density between G and C obtained by numerical simulation for experimental condition from figure 5

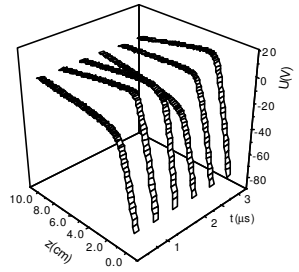

Fig. 7: Axial distribution of electrostatic potential between G and C obtained by numerical simulation

Numerical simulations using the PDP1 code and similar parameters as in the experiment show similar results as those presented in Fig. 6. The ion space charge is forming at a distance of about 1cm from the grid. The axial distribution of the electrostatic potential is also presented in Fig. 7, which is also similar to the distributions measured by emissive probes and presented in [11].

Acknowledgments

This work was partly financed by the Romanian CNCIS Grant no. 39.699/1998 and supported by the Fonds zur Förderung der wissenschaftlichen Forschung (Austria) under Proj. No. P-12145 and by the University of Innsbruck, and has been part of the Association EURATOM-ÖAW under contract no. ERB 5004 CT 960020.

References

[1] T.C. Frey, *Phys Rev.* **17**, 441 (1921)
[2] I. Langmuir, *Phys. Rev.*, **21**, 419 (1923)
[3] P. Auer, *J. Appl. Phys.*, **31**, 2096 (1960)
[4] A.L. Fichenbann and K.G. Hennqvist, *J. Appl. Phys.*, **32**, 16 (1962)
[5] W.T. Norris, *J. Appl. Phys.*, **35**, 3260 (1964)
[6] W.H. Cutler and P. Burger, *J. Appl. Phys.*, **37**, 2867 (1966)
[7] R.W. Motley, *Q-machines* (Academic, NY, London, 1975)
[8] S. Kuhn, *Plasma Phys.*, **23**, 881 (1981)
[9] S.V. Bulanov, S. Kuhn and A.S. Sakharov, *Phys. Fluids*, **B4**, 2871 (1992)
[10] M. Morhagen and S. Kuhn, *Phys. Fluids*, **B2**, 2741 (1980)
[11] G. Popa and R. Schrittwieser, *Phys. Plasmas*, **1** (1994) 32.
[12] A. Vizir, E. M. Oks, I.G. Brown, *IEEE Trans. On Plasma Sci., **26**, 1353 (1998).*